arXiv:astro-ph/0204365v1 22 Apr 2002

Optical and Radio monitoring of S5 1803+784

R. Nesci, E. Massaro, M. Maesano, F. Montagni, S. Sclavi

Dipartimento di Fisica, Universitá La Sapienza, P.le A. Moro 2, 00185, Roma, ITALY

Roberto.Nesci@uniroma1.it

T. Venturi, D. Dallacasa

Istituto di Radioastronomia CNR via P. Gobetti 101, I-40129 Bologna, Italy

tventuri@ira.bo.cnr.it

and

F. D'Alessio

Osservatorio Astronomico di Roma, via di Frascati 33, Monteporzio Catone I-00040, Italy

dalessio@coma.mporzio.astro.it

ABSTRACT

The optical (BVRI) and radio (8.4 GHz) light curves of S5 1803+784 on a time span of nearly 6 years are presented and discussed. The optical light curve showed an overall variation greater than 3 mag, and the largest changes occured in three strong flares. No periodicity was found in the light curve on time scales up to a year. The variability in the radio band is very different, and shows moderate oscillations around an average constant flux density rather than relevant flares, with a maximum amplitude of $\sim$30%, without a simultaneous correspondence between optical and radio luminosity. The optical spectral energy distribution was always well fitted by a power law. The spectral index shows small variations and there is indication of a positive correlation with the source luminosity. Possible explanations of the source behaviour are discussed in the framework of current models.

Subject headings: BL Lacertae objects: individual (S5 1803+784), Galaxies: Active, Galaxies: Photometry

1. Introduction

The radio source S5 1803+784 was classified as a BL Lac object by Biermann et al. (1981). A redshift estimate (0.680) was derived from a weak MgII line by Lawrence et al. (1996) and recently confirmed by Rector & Stocke (2001). From the available flux measurements, although non simultaneous, the overall energy distribution from radio to the X rays (in the Log (νF_ν) *vs* Log (ν) plot) peaks in the IRAS band (Giommi et al. 1995), so that the source is classified as a Low Energy Peaked BL Lac (LBL) object in the scheme proposed by Padovani & Giommi (1995). Like other sources of this class, one would expect in the optical band a remarkable variability with a correlation between the spectral slope and the luminosity (see e.g. Massaro et al. 1999; Nesci et al. 1998). The published photometric data, however, are very few: Wagner et al. (1990) and Heidt & Wagner (1996) reported only uncalibrated luminosity variations relative to a few weeks, and practically nothing is known about the long term time behaviour of the source. Only in the radio band S5 1803+784 was extensively monitored, both from the group of the University of Michigan (Aller et al. 1998) and from the Metsahovi observatory (Teraesranta et al. 1998), while several VLBI images have been obtained at different epochs since 1979 (Biermann et al. 1981), because it is normally used as a reference radio source for geodynamics studies (see Britzen et al. 1999; Gabuzda 1999, 2000).

In April 1996 we started an optical monitoring program to define the long term light curve and color variations of this source. A parallel radio monitoring program at 5 GHz and 8.4 GHz was carried out starting from January 1996 with the two 32-m antennas located in Medicina (Bologna, Italy) and Noto (Siracusa, Italy), as part of a larger project to provide radio lightcurves of several bright BL Lac objects, possible targets of X-ray observations (Venturi et al. 2001). In this paper we present the observational results of this monitoring and discuss some implications of our measures on the nature of the luminosity changes. The observational data are described in Section 2; the light-curve temporal analysis is discussed in Section 3; the optical spectral distribution is discussed in Section 4; the general discussion of the results is made in Section 5.

2. Observations

2.1. Optical observations

The large majority of our observations were made with a 50 cm f/4.5 telescope at the Vallinfreda astronomical station near Rome (850 m a.s.l.), equipped with a CCD camera based on the Texas TC241 chip. A minor number of data were collected with a 32 cm f/4.5

telescope located at Greve (Tuscany, 650 m a.s.l.) and a 70 cm f/8.3 telescope at Monte Porzio (Roma, 380 m a.s.l.) both equipped with the same model of CCD camera, based on the SITe SIA501A back-illuminated chip. The filter sets of all these telescopes are identical and match the standard B,V (Johnson) and R,I (Cousins) bandpasses. The typical exposure times were 300 s for the V,R,I bands and 600 s for the B band. When the source was faint (for R>16 mag) exposure times were doubled.

Systematic differences between the data sets of the three observatories were checked during several observational campaigns of BL Lac objects using simultaneous, or nearly simultaneous observations, and found to be negligible. For S5 1803+784, in particular, we have two nights in common between Vallinfreda and MontePorzio, two nights between Vallinfreda and Greve, and one night between Greve and Vallinfreda. Bias, dark and flat field corrections of the frames were performed with IRAF tasks, and aperture photometry was made with IRAF-apphot, using an aperture of 5 arcsec radius. Local background level was estimated from an annular region concentric to each star.

Magnitudes of S5 1803+784 were estimated differentially with respect to five nearby reference stars. The final results, listed in Table 3, are the average of the magnitude differences with respect with the reference stars, and the quoted error is the standard deviation of the single measures. The intercalibration of these five stars, in each filter, was made using the best 35 nights. Their magnitude differences agreed with a standard deviation of 0.01 magnitudes in each filter. No evidence of variability of these stars was detected in all our database.

The zero point calibration for each photometric band was made linking the brightest reference star (Star A in Table 1) to the photometric sequences of five other BL Lac objects, namely PKS 0422+004 (Miller et al. 1983); AO 0235+164 (Smith et al. 1985, McGimsey et al. 1976, Rieke et al. 1976; 3C66A (Fiorucci & Tosti 1996); S5 0716+714 (Ghisellini et al. 1997); BL Lacertae (Bertaud et al. 1969, Fiorucci & Tosti 1996). For this purpose the best photometric nights were used, with air masses ranging from 1.0 to 1.5. The number of nights used for each filter is listed (in round bracketts) in Table 1.

For each filter and night a linear fit of the extinction law was derived and used to convert the instrumental magnitudes into the apparent ones. The final result is the average over the different nights, and the error is the standard deviation of the mean. Given the large errors found in deriving the calibration of the reference stars in the B band, a new calibration of star A was made using four Bright Stars (HR 6598, 6636, 6637 and 6811). Their B magnitudes were taken from the Bright Star Catalogue, 5th Revised Edition, as given at the CDS (Hoffleit & Warren 1991). The results are reported in Table 1: the errors quoted for star A include the zero point uncertainty, while those for the other stars are the

intercalibration standard errors of the mean, derived from the average of 35 images for each colour. The finding chart is shown in Fig. 1.

From the digitized Palomar sky survey plates and using our photometric sequence, we also derived a few approximate historical magnitudes for S5 1803+784, which are collected in Table 2.

2.2. Optical light curve

In total we collected data for 207 days, 85 with full BVRI photometry and further 49 with VRI photometry, since April 1996 until January 2002. The whole data set is given in Table 3 and the R light curve is shown in Fig. 2: typical errors are 0.02-0.03 mag when the source was bright and 0.06 when very faint.

Until JD 2451350 (Sep. 1999), the source behavior can be simply described as a monotonic increase of the luminosity, with small (0.3 mag) amplitude and relatively fast variations above or below the average level, with three strong bursts at JD 711, 1127 and 1344 (hereafter we report the JD dates minus 2450000) of comparable amplitude and time scale. In the last event the source reached its highest recorded level (R=14.0). Then a decay phase started, with still some oscillations overimposed, bringing the flux of S5 1803+784 at the lowest recorded level (R$\sim$17.4, July 2001). After that a new rising phase started. The overall magnitude interval is therefore about 3.4 mag, confirming a large optical variability, typical of this class of BL Lac objects.

The three largest bursts indicated above are reported enlarged in Fig. 3, 4 and 5. For ease of comparison, the same scales were used for all three Figs. The V$-$I colour index is also plotted, with the scale marked on the right hand side.

The first episode (Fig. 3) was observed only in the decreasing branch and showed a monotonic decline of 1.4 mag in 20 days, with a mean rate of 0.07 mag/day. Because of the sampling only a lower limit of 0.036 mag/day can be set to the rate of the rising branch. In the second one (Fig. 4), one can see a rise by 1.5 mag in 21 days (0.071 mag/day). The subsequent decrease was initially fast, with approximately the same time scale of the increase; after, our data indicate a change of the slope. In the third event (Fig. 5) the source reached its brightest state and likely it remained so bright for about one month, then a decline phase started of about 1.7 mag in 78 days.

The greatest variation rate, derived from this inspection of the main events, is therefore 0.07 mag/day, observed both in rising and in decaying segments. Given the uneven sampling

of the light curve we cannot exclude rates greater than this estimate, but such rates might have lasted only on very short (day) time scale. We think however that very fast variations, if present, do not represent the normal behavior of the source and the above estimate can be used to give constraints to theoretical models of variability mechanisms.

2.3. Near Infrared observations

Observations in the Johnson JHK bands were performed in August 2001 with the AZT24 telescope at Campo Imperatore (110 cm f/7.9, Cassegrain) and a PICNIC type HgCdTe 256x256 camera, with a scale of 1 arcsec/pixel. Each image was the sum of 6 individual frames of 30s exposure, to avoid saturation. Preliminary data reduction was made with the PREPROCESS task developed at the Roma Observatory, and photometry was made with IRAF/daophot using a 4 arcsec radius aperture. Primary photometric standard stars (AS02, AS06, AS32, AS37-1) were taken from Hunt et al. (1998). All the observations were made at airmass smaller than 1.2; the standard error of our JHK observations is $\sim$0.05 mag. The results are collected in Table 4. Simultaneous optical photometry was obtained with the Vallinfreda telescope.

2.4. Radio observations

The 4-year radio monitoring of S5 1803+784 was carried out at 5 GHz and 8.4 GHz with the 32-m antennas located in Medicina (Bologna, Italy) and Noto (Siracusa, Italy) on monthly basis, starting from January 1996. The observations were performed by means of ON-OFF measurements on the target source. The systematic calibration uncertainty of the absolute radio flux is of the order of 4%, while the typical inner error of the measurements is 10 - 20 mJy. Details on the observations and data reduction can be found in Venturi et al. (2001). The 8.4 GHz data (the more complete dataset in our radio monitoring) are shown in Fig. 6, upper panel; for ease of comparison the optical data are shown in the lower panel of the same figure.

The radio light curve shows a significant variability around an average flux density of 3 Jy. The minimum measured flux was 2.46 $\pm$0.02 Jy on JD 657 and the maximum was 3.46 $\pm$0.01 on JD 1376. The sampling is much coarser than the optical one, so that a cross correlation analysis would not be very meaningful: a simple eye-comparison of the two light curves does not suggest anyway a simultaneus correspondence between them. We note however that simultaneous radio-optical measurements on July 12 2001 (JD 2103), when the

source was near its minimum optical brightness, gave radio flux densities of $F_{8.4} = 2.53$ Jy (and $F_{5.0} = 2.50$ Jy at 5 GHz on July 17), one of the lowest recorded radio levels in our monitoring.

The amplitude of the radio variability seems to increase from 1997 to 2000: the flux density difference between maxima and minima going from ~ 0.2 Jy (i.e. $\sim 7\%$) at the beginning of 1997 to 0.8 Jy (i.e. $\sim 28\%$) in 1999-2000.

3. Time scale analysis

The search for possible time scales in the optical light curve was performed by means of the Discrete Fourier Transform (DFT) for unevenly spaced data (Deeming 1975). We also used the Structure Function (SF) analysis (Simonetti et al. 1985) and the Jurkevich (1971) method.

The DFT power spectrum is plotted in Fig. 7: the upper panel shows the light curve spectrum, and the lower panel that of the sampling window. The former spectrum is clearly dominated by a very prominent maximum at the lowest frequency due to the long term trend; a few other peaks are also present, two of them corresponding to the periods of about 218 and 105 days. The first period is nearly the distance between the second and the third flare. The latter could be just the first harmonic of 218, given the achievable resolution step. Note that in the window power spectrum a feature is present at 105 days, and therefore this frequency in the source power spectrum could be enhanced by the convolution effect. None of these features in the power spectrum, however, is so prominent to suggest a stable periodicity. The window power spectrum shows a marked periodicity at $\sim$29 days, corresponding to the moon phase period.

Application of the Jurkevich test for the search of periodicities was made starting with a trial period of 5 days, and increasing it with a 5 days step, binning into 29 intervals the phase-reduced light curve. Given our average sampling of about 1 point every 10 days, shorter time scales cannot be explored with our database, save that in a few short intervals of denser sampling. For a better detection of possible time scales, we subtracted from the R light curve the average trend, derived with the running mean over 5 consecutive values. The result of the Jurkevich test is shown in Fig. 8, where the f parameter is plotted against the trial period. We recall that f is defined as 1-V_B/V_T, where V_B is the sum of the variances of the phase-reduced binned data and V_T is the variance of the whole sample. Minima in this plot may be considered as indicators of possible time scales: a value of f smaller than $\sim$0.5 is often quoted in the literature as indicator of a 'true' time scale (e.g. Kidger, Takalo &

Sillanpää 1992). Several minima appear in this plot, the shortest one around 620 days (close to the lag between the first and the third flare), but all of them are far from the significancy threshold. Changing the number of bins and the step of the trial periods does not change substantially the positions of the minima, nor their relative depth.

Finally the SF plot, averaged over a logaritmic time window of 0.1, is shown in Fig. 9. It has been calculated on the flux density values in mJy and no normalization has been applied. The SF has an average slope of 0.62±0.04 in the time lag range between 10 and 1000 days. A plateau region is marginally apparent between 20 and 80 days. No clear periodicity, which would reveal as a local minimum, is present. On short time scales (days) the SF analysis for S5 1803+784 was previosly studied by Heidt & Wagner (1996) for two different observing runs, and for time lags greater than 1 day they report a slope of 0.58±0.13 practically coincident with our result.

In Fig. 9 we also report the SF for the radio light curve at 8.4 GHz, calculated on the flux densities in Jy, with the same binning of the optical one, again without any normalization. The points are more scatted than the optical ones but the mean slope is not significantly different (0.51±0.18). No indication of periodicity is evident also in the radio data.

4. Optical energy distribution

Besides the R band, most of the times also B, V and I band observations were secured, to allow the determination of the broad band shape of the energy distribution. Plots of the color indices B−V, V−R and R−I as a function of time are reported in Fig. 10. Their average values are B−V=0.59±0.05, V−R=0.49±0.04 and R−I=0.63±0.03, where the quoted errors are 1 σ deviations of the data set. Large systematic changes of the source colour are not evident, in particular during the three large luminosity variations episodes (see Figs. 3 to 5).

Several BL Lac objects have optical spectra well reproduced by a power law ($F_\nu = A\nu^\alpha$). To derive the spectral index it is necessary to correct the observed fluxes for the foreground absorption, which is expected to be not very large, given the relatively low (b=29 degrees) galactic latitude of this source. We evaluated the absorption from literature N_H values (3.90×10^{20}, Ciliegi et al. 1995; 3.70×10^{20}, Murphy et al. 1996), and adopting the ratio N_H/E(B−V) = 5.2×10^{21} cm^{-2}mag^{-1} from Shull & Van Steenberg (1985). The resulting colour excess E(B−V)=0.075 was derived, and the corresponding extinctions in the B, V, R, I bands computed assuming the curve by Schlegel et al. (1998). Conversion from magnitudes to fluxes was made according to Mead et al. (1990). Any contribution from the host galaxy is

likely negligible, given that the CaII break is undetectable in the published spectra (Lawrence et al. 1996; Rector & Stocke 2001).

We have 85 4-band simultaneous observations of this source, useful to derive the spectral index. A fit of $\log(F_\nu)$ vs $\log(\nu)$ with a straight line of slope α gives a satisfactory result against a χ^2 test for nearly all our simultaneous 4-bands observations, supporting the power law modelling of the spectral energy distribution. We report in Table 4 the JD, R, $\sigma(R)$, α, $\sigma(\alpha)$ and χ^2 for each day. Consistent results are obtained using the larger set (134) of good quality V, R, I simultaneous observations. Our average value (-1.54, with a dispersion of 0.12) is in good agreement with the result of the only spectrophotometric observation of S5 1803+784 available in the literature (-1.48; Lawrence et al., 1996). A plot of the spectral index *vs* the R magnitude is shown in Fig. 11. The linear correlation coefficient was found equal to 0.42, which means a probability less than 10^{-3} that the correlation is merely due to chance. From this plot it is apparent however that at relatively large changes of the luminosity do not correspond large variations of the spectral slope, at variance with other BL Lac objects, like ON 231 (Massaro et al. 1999) or BL Lacertae (Nesci et al. 1998).

5. Discussion

In this paper we presented the first flux calibrated, long term variability study of the BL Lac object S5 1803+784 in the optical frequency range, spanning more than five years since Spring 1996. Furthermore, we made a comparison with the behaviour of this source in the same period in the radio band at 8.4 GHz.

The main results can be summarized as follows:

a) the source showed an optical luminosity variation with an amplitude of a factor $\sim$ 20;

b) the general behaviour was characterized by an increase of the mean flux level for at least 1150 days during which we observed with three large flares, followed by a decrease in about 400 days down to a much lower state;

c) there is no evidence of periodicity in the light curve on the time scales (several months) well sampled by our dataset;

d) the three major flares were characterized by comparable rise and decay times of about 20 days, corresponding to an (unbeamed) dimension of the emitting region $R \simeq c\Delta t \simeq 5 \times 10^{16}$ cm;

e) changes of the source luminosity are not related to strong systematic trends of the spectral slope α. A correlation test provided evidence for an increase of the slope in fainter states: however the α values corresponding to the highest and lowest luminosity differ only by $\sim$0.1 while larger differences were occasionally found in intermediate states;

f) the source showed variability in the radio band, with maximum to minimum difference of 1 Jy and a mean flux density value of $\sim$3 Jy at 8.4 GHz.

The slopes of the optical spectrum, derived in Section 3, indicate that the synchrotron emission peak of the SED should be in the IR range. The only JHK photometric data available in the literature are those by Heckman et al. (1983) taken in 1980-81 and give a much flatter slope (about -0.8). The IRAS data (Impey & Neugebauer 1988) give a substantially flat energy distribution suggesting that the SED should peak between 10 and 100 μm.

To derive a more complete SED we retrieved from the ISOCAM archive the four available calibrated images, taken in April 1996 but still unpublished, and made a simple aperture photometry. In the X ray band, the source was lately observed by BeppoSAX on 28-Sep-1998 (Padovani et al. in preparation). The 2-10 keV spectrum had an energy spectral slope α_x=-0.45, significantly flatter than the optical one (-1.7), indicating that the X-ray emission was completely dominated by the Inverse Compton component. Our nearest optical data are on 20-Sep and 11-Oct giving the source respectively at R=15.3 and R=15.7 (see Table 3).

Using these data, although not simultaneous, we constructed the SED, given in Fig. 12, which improves on that given by Giommi et et. (1996). For our optical and radio monitoring we plotted only the minimum and maximum values, to give a feeling of the variability of the source. For the JHK bands we plotted our data, together with the simultaneous optical ones. The R value form our monitoring simultaneous to the ISOCAM observation is also plotted. The general impression of a peak of the SED in the infrared range is confirmed from Fig. 12.

It is interesting to compare the luminosity and the behaviour of S5 1803+784 with that of other BL Lac sources at their maximum luminosity. At the highest level (R=14), adopting H_0=65 km s^{-1} Mpc^{-1} and q_0=0.5, the absolute magnitude of the source is M$_R$=$-$28.7, corresponding to an integrated optical luminosity of 3.6 10^{46} erg s^{-1}. ON 231, which reached the highest recorded flux (R=12.2) in Spring 1998 (Massaro et al. 1999), at a redshift $z = 0.10$, reached an absolute luminosity M=$-$26.2, i.e. 2.5 mag weaker than S5 1803+784. BL Lac, during the large flare in 1997 (Bloom et al. 1997) reached R=12.3, corresponding to M=$-$25.2, i.e. 3.5 mag fainter than S5 1803+784. These different absolute luminosities

may be due to an intrinsic different power or to a different beaming factor. Lähteenmäki & Valtaoja (1999) estimated Doppler boosting factors δ from variations of brightness temperature at 22 and 33 GHz and found values of 1.6 for ON 231, 3.9 for BL Lac and 6.5 for S5 1803+784. The higher beaming could be the reason of the apparent higher luminosity of our source: however, in this case, the higher time contraction would imply large amplitude flux variations on quite short time scales, which have not been detected in our observation, at variance with ON 231 and BL Lac (Nesci et al. 1998).

We can also estimate the unbeamed luminosity using the factor δ given above, and from the relation

$$L_{obs} = \delta^{(3-\alpha)} L_{unb}, \quad (1)$$

we obtain an intrinsic optical luminosity of 7.8 10^{42} erg/s, which is quite reasonable (Cavaliere & Malquori 1999).

A simple radiative cooling mechanism of freshly accelerated electrons cannot explain the color behaviour of the bright flares of S5 1803+784, in particular that on JD 711: in fact one would expect a significant steepening of the spectral slope in the dimming phase, like that clearly detected in the flares of ON 231 (Massaro et al. 1999) which is not the case. A possible explanation would be that the observed spectral shape is the result of an equilibrium condition between acceleration and radiation processes, while the total number of particles involved, which determine the flux level, changes with time. In this case however one should invoke that the injection and leakage time scales must be similar. An alternative possibility is that the flares are originated by a change of δ. Being the flux proportional to $\delta^{(3-\alpha)}$ a variation of Δm magnitudes would require a variation of δ according to the relation:

$$log(\delta_2/\delta_1) = 0.4(m_1 - m_2)/(3 - \alpha), \quad (2)$$

which for $\alpha \sim -1.5$ implies a variation of δ by a factor 1.5 for $\Delta m = 2$, which looks rather substantial.

ACKNOWLEDGEMENTS

The criticisms of an anonimous referee has helped to improve the first version of this paper. Part of this work was supported by the Italian Ministry for University and Scientific Research (MURST) with grant Cofin-98-02-32 and Cofin 2001/028773. This research has also made use of the NASA/IPAC Extragalactic Database (NED) which is operated by the Jet Propulsion Laboratory, California Institute of Technology, under contract with the

National Aeronautics and Space Administration.

REFERENCES

Aller M.F., Aller H.D., Hughes P.A. and Latimer G.E., 1998, ApJ, 512, 601

Bertaud C., Dumortier B., Veron P. 1969 A&A, 3, 436

Biermann P., Duerbeck H., Eckart A., Fricke K., Johnston K.J. et al. 1981, ApJ, 247, L53

Bloom S.D, Bertsch D.L., Hartman R.C. et al. 1997 ApJ, 490, L145

Britzen S., Witzel A., Krichbaum T.P., Muxlow T.W.B. 1999, New Astr. Rev. 43,751

Cavaliere A. and Malquori D, 1999 ApJ, 516, L9

Ciliegi P., Bassani L., Caroli E., 1995 ApJ, 439, 80

Deeming T.J., 1975, Ap&SS, 36, 137

Fiorucci M. and Tosti G. 1996, A&AS, 116, 403

Gabuzda D.C., 1999, New Astron. Rev., 43, 691

Gabudza D.C. 2000, in Astrophys. Phenomena Revealed by Space VLBI, H. Hirabayashi, P.G. Edwards and D.W. Murphy eds.

Ghisellini G., Villata M., Raiteri C. et al. 1997 A&A, 327, 61

Giommi P., Ansari S.G., Micol A. 1995, A&AS, 109, 267

Heidt J. and Wagner S.J. 1996, A&A, 305, 42

Heckman T.M., Lebofsky M.J. Rieke G.H. van Breguel W. 1983, ApJ, 272, 400

Hoffleit E.D., Warren jr. W.H. 1991, Bright Star Catalogue 5th revised edition, Centre de Donnee astronomiques de Strasbourg.

Hunt L.K., Mannucci F., Testi L. et al. 1998, AJ, 115, 2594

Jurkevich I., 1971, Ap&SS, 13, 154

Impey C.D. and Neugebauer G., 1988, AJ, 95, 307

Kidger M., Takalo L. and Sillanpää A., 1992, A&A, 264, 32

Lähteenmäki A. & Valtaoja E. 1999, ApJ, 521, 493

Lawrence C. R., Zucker J. R., Readhead A. C. S. et al. 1996, ApJS, 107, 541

Massaro E., Nesci R., Maesano M., Montagni F., Trevese D. et al A&A, 314, 87

Massaro E., Maesano M., Montagni F., Nesci R., Tosti G. et al. 1999, A&A, 342, L49

Mc Gimsey G.Q., Miller H.R., Williamon R.M. 1976 ApJ, 81, 750

Mead A.R.G., Ballard K.R., Brand P.W.J.L. et al. 1990, A&AS83, 183

Miller H.R., Mullikin T.L., McGimpsey B.Q. 1983, ApJ,

Murphy E.M., Lockman F.J., Laor A., Elvis M., 1996, ApJS, 105, 369

Nesci R., Maesano M., Massaro E., Montagni F., Tosti G., 1998, A&A, 332, L1

Padovani P. and Giommi P. 1995, ApJ, 444, 567

Padovani P. et al. in preparation

Rector T.A. and Stocke J.T. 2001, AJ, 122, 565

Rieke G.H., Grasdalen G.L., Kinman T.D., Hintzen P., Wills P.J., Wills D., 1976, Nature 260, 754

Schlegel D.J., Finkbeiner D.P. and Davis M., 1998, ApJ, 500, 525

Simonetti J.H., Cordes J.M., Heeschen D.S., 1985, ApJ, 296, 46

Shull, J. M., van Steenberg, M. E. 1985, ApJ, 294, 599

Smith P.S., Balonek T.J., Heckert P.A., Elston R., Schmidt G.D. 1985 AJ, 90, 1184

Teraesranta H., Tornikosky M., Mujunen A., et al. 1998, A&AS, 132, 305

Venturi T., Dallacasa D., Orfei A., Bondi M., Fanti R. et al. 2001, A&A, 379, 755

Wagner S.J., Sanchez-Pons F., Quirrenbach A., and Witzel A., 1990, A&A, 235, L4

This preprint was prepared with the AAS LaTeX macros v5.0.

Fig. 1.— The finding chart of S5 1803+784 from the POSS-I 103aE plate. Reference stars are marked according to Table 1; the blazar is marked with S.

Fig. 2.— The R_C light curve of S5 1803+784 from Apr 1996 to Jan 2002.

Fig. 3.— First flare. The R light curve (filled boxes) and the V−I colour index (crosses with error bars). The colour index scale is on the right side, the R magnitude scale is on the left. No appreciable variation of the V−I colour index is present.

Fig. 4.— Second flare. The R light curve (filled boxes) and the V−I colour index (crosses with error bars). Scales as in Fig.3

Fig. 5.— Third flare. The R light curve (filled boxes) and the V−I colour index (crosses with error bars). Scales as in Fig. 3. Marginal evidence for a redder colour in the decreasing branch is present.

Fig. 6.— The radio light curve of S5 1803+784 at 8.4 GHz since 1996 (upper panel), and the R light curve in linear scale (mJy) not corrected for reddening (lower panel).

Fig. 7.— Power spectra of the light curve (upper panel) and of the sampling window (lower panel). The peaks corresponding to 218 and 105 days are indicated.

Fig. 8.— The Jurkevich test for 5 days step periods.

Fig. 9.— The structure function for the optical data, averaged over $\log(\Delta t_{days})$=0.1 (filled squares) and of the radio data averaged in the same way (open circles). No normalization has ben applied to the data.

Fig. 10.— B−V, V−R and R−I colour indices plotted as a function of time. Some data with large errors have been omitted.

Fig. 11.— The 4-band spectral index as a function of the R magnitude. The linear correlation coefficient is 0.42.

Fig. 12.— The spectral energy distribution of S5 1803+784 derived from literature and our measurements: NED data (radio and IRAS), open squares; radio data (max and min, this paper), filled squares; ISO and simultaneous optical data, filled triangles; simultaneous NIR and optical data (this paper), open triangles; optical data (max and min, this paper), filled circles; BeppoSAX x-ray data, crosses.

Table 1. Magnitudes of comparison stars for S5 1803+784.

Star[a]	B	V	R	I
A	15.39±.05 (7)	14.54±.03(8)	14.06±.03(10)	13.62±.03(8)
B	15.97±.01	15.30±.01	14.92±.01	14.53±.01
C	16.37±.01	15.73±.01	15.36±.01	14.97±.01
D		16.58±.01	16.08±.01	15.57±.01
E		16.49±.01	16.10±.01	15.70±.01

[a]Errors for star A include the zero point uncertainty, while for the others only the intercalibration uncertainty is given

Table 2. Photographic archive magnitudes of S5 1803+784.

Band	mag	date	Survey	emulsion
R	14.5	11-08-1953	POSS-I	103aE
V	15.5	16-05-1983	Quick Blue	IIaD
R	15.5	21-08-1993	POSS-II	IIIaF
B	16.6	12-09-1993	POSS-II	IIIaJ

Table 3. B,V,R,I magnitudes of S5 1803+784.

JD[a]	B	σB	V	σV	R	σR	I	σI	Tel
193.4382	0.00	0.00	16.53	0.05	15.96	0.03	15.38	0.03	VA
222.4194	0.00	0.00	0.00	0.00	15.93	0.03	0.00	0.00	VA
246.4236	0.00	0.00	0.00	0.00	15.76	0.02	0.00	0.00	MP
272.4507	0.00	0.00	16.87	0.03	0.00	0.00	15.73	0.03	VA
277.5292	0.00	0.00	17.03	0.05	16.55	0.05	15.90	0.03	VA
354.4250	0.00	0.00	16.28	0.06	15.82	0.03	0.00	0.00	VA
357.3854	0.00	0.00	0.00	0.00	15.87	0.02	0.00	0.00	VA
375.3771	0.00	0.00	16.67	0.03	16.21	0.03	0.00	0.00	VA
377.3847	0.00	0.00	16.67	0.03	16.24	0.03	15.55	0.05	VA
378.4056	0.00	0.00	16.64	0.03	16.19	0.03	15.53	0.03	VA
381.2625	0.00	0.00	16.60	0.03	16.19	0.03	0.00	0.00	VA
390.3125	0.00	0.00	16.61	0.05	16.16	0.05	0.00	0.00	VA
391.2313	0.00	0.00	16.60	0.03	16.18	0.05	0.00	0.00	VA
415.3014	0.00	0.00	16.27	0.03	15.82	0.04	15.18	0.03	VA
421.2299	0.00	0.00	16.57	0.03	16.11	0.03	0.00	0.00	VA
464.2500	16.67	0.03	16.16	0.03	15.71	0.03	15.04	0.03	VA
476.3542	0.00	0.00	15.86	0.03	15.43	0.03	14.86	0.03	VA
487.5382	0.00	0.00	15.98	0.03	15.48	0.03	14.83	0.03	VA
488.6021	0.00	0.00	16.01	0.03	15.52	0.04	14.90	0.03	VA
517.4750	0.00	0.00	16.40	0.03	15.94	0.04	15.24	0.03	VA
521.4507	0.00	0.00	0.00	0.00	15.64	0.04	15.12	0.03	VA
549.4910	16.93	0.06	16.34	0.03	15.85	0.03	15.23	0.03	VA
572.4729	0.00	0.00	15.57	0.03	15.02	0.03	14.38	0.03	VA
598.5042	0.00	0.00	15.98	0.03	15.50	0.03	0.00	0.00	VA
628.4424	0.00	0.00	0.00	0.00	15.67	0.03	0.00	0.00	VA
639.4271	0.00	0.00	16.49	0.03	16.00	0.03	15.29	0.03	VA
669.3965	0.00	0.00	16.42	0.03	15.94	0.03	0.00	0.00	VA
711.3493	15.44	0.05	14.90	0.03	14.43	0.02	13.76	0.03	VA
712.2597	15.61	0.05	15.09	0.03	14.54	0.03	13.87	0.03	VA
717.2931	15.65	0.03	15.03	0.04	14.54	0.03	13.92	0.03	VA
719.2528	15.84	0.03	15.30	0.03	14.77	0.03	14.11	0.03	VA
721.3368	15.91	0.04	15.38	0.03	14.82	0.03	14.19	0.03	VA
723.2437	16.02	0.05	15.57	0.03	15.06	0.03	14.43	0.03	VA
723.4479	15.97	0.04	15.51	0.03	14.99	0.03	14.37	0.03	VA
725.3299	0.00	0.00	0.00	0.00	15.15	0.02	0.00	0.00	VA
727.3264	16.77	0.03	16.04	0.03	15.51	0.03	14.88	0.03	VA
731.3243	16.93	0.04	16.26	0.04	15.78	0.03	15.13	0.03	MP
739.2917	0.00	0.00	16.30	0.04	15.82	0.03	15.18	0.03	VA
742.2708	0.00	0.00	0.00	0.00	15.64	0.03	0.00	0.00	VA
744.2792	16.64	0.04	16.06	0.03	15.51	0.03	14.88	0.03	VA
747.2549	16.46	0.03	15.90	0.03	15.40	0.04	14.78	0.03	VA
748.3292	16.46	0.03	15.93	0.03	15.39	0.03	14.75	0.03	VA
756.2889	0.00	0.00	15.92	0.03	15.44	0.03	14.82	0.03	VA
781.2681	16.99	0.09	16.28	0.02	15.70	0.03	15.09	0.03	MP
791.2174	0.00	0.00	0.00	0.00	15.27	0.03	0.00	0.00	VA
823.2160	16.12	0.05	15.62	0.03	15.11	0.03	14.45	0.03	VA
825.2132	0.00	0.00	15.55	0.03	15.04	0.03	14.37	0.03	VA
832.2194	0.00	0.00	15.89	0.04	15.35	0.02	14.75	0.02	VA
838.2549	0.00	0.00	16.13	0.04	15.55	0.02	14.92	0.02	VA

Table 3—Continued

JD[a]	B	σB	V	σV	R	σR	I	σI	Tel
840.2556	0.00	0.00	16.15	0.03	15.69	0.01	15.02	0.02	VA
842.2257	0.00	0.00	16.14	0.03	15.63	0.02	14.96	0.03	VA
843.2250	0.00	0.00	16.20	0.02	15.63	0.01	15.02	0.04	VA
858.2444	16.65	0.08	0.00	0.00	15.55	0.02	0.00	0.00	VA
860.2382	0.00	0.00	16.02	0.02	15.53	0.02	14.85	0.03	VA
862.2472	0.00	0.00	16.21	0.02	15.58	0.01	14.87	0.01	VA
863.2597	16.58	0.06	16.09	0.03	15.53	0.01	14.83	0.01	VA
865.5174	16.55	0.05	15.98	0.02	15.40	0.01	14.74	0.01	VA
871.5194	16.28	0.03	15.71	0.02	15.11	0.01	14.57	0.01	VA
872.4646	16.37	0.02	15.75	0.01	15.15	0.01	14.59	0.05	VA
891.4333	16.40	0.04	15.84	0.02	15.28	0.01	14.62	0.01	VA
895.5132	0.00	0.00	15.89	0.02	15.36	0.01	14.68	0.01	VA
900.3889	0.00	0.00	15.89	0.02	15.37	0.02	0.00	0.00	VA
901.4056	16.59	0.05	15.89	0.03	15.46	0.02	14.71	0.02	VA
907.4604	0.00	0.00	0.00	0.00	15.33	0.02	0.00	0.00	VA
924.5722	0.00	0.00	15.37	0.02	14.83	0.01	14.20	0.01	VA
928.4799	15.91	0.07	15.45	0.02	14.90	0.01	14.26	0.01	VA
942.3563	0.00	0.00	0.00	0.00	15.10	0.04	0.00	0.00	VA
947.4076	0.00	0.00	15.46	0.04	14.93	0.03	0.00	0.00	VA
950.4188	0.00	0.00	0.00	0.00	14.67	0.01	14.02	0.04	VA
953.4444	0.00	0.00	15.48	0.02	14.90	0.02	0.00	0.00	VA
955.4368	15.86	0.03	15.31	0.03	14.82	0.01	14.10	0.01	VA
956.4264	15.70	0.04	15.12	0.05	14.54	0.01	13.96	0.01	VA
966.3799	0.00	0.00	15.15	0.01	14.64	0.02	14.06	0.01	VA
970.4146	0.00	0.00	15.86	0.04	15.26	0.03	14.57	0.02	VA
983.4451	0.00	0.00	15.97	0.03	15.45	0.01	14.77	0.02	VA
985.4597	16.53	0.02	15.91	0.01	15.38	0.02	14.73	0.01	VA
988.4215	0.00	0.00	15.86	0.05	15.39	0.02	14.70	0.02	VA
993.4562	16.03	0.01	15.48	0.01	14.94	0.01	14.34	0.01	VA
997.5181	0.00	0.00	15.17	0.03	14.71	0.01	14.11	0.01	VA
1001.4118	15.64	0.02	15.06	0.02	14.64	0.02	14.03	0.02	VA
1004.3958	15.79	0.02	15.28	0.02	14.78	0.02	14.23	0.02	VA
1005.3806	16.01	0.04	15.42	0.02	14.97	0.02	14.38	0.02	VA
1008.3944	16.07	0.02	15.52	0.04	15.11	0.02	14.47	0.03	VA
1011.4000	0.00	0.00	15.50	0.02	15.04	0.01	14.44	0.02	VA
1013.3979	15.98	0.03	15.39	0.02	14.94	0.01	14.41	0.02	VA
1015.3826	0.00	0.00	15.38	0.02	14.89	0.02	0.00	0.00	VA
1016.4271	0.00	0.00	15.35	0.04	14.87	0.03	14.25	0.03	GR
1018.3799	15.91	0.02	15.38	0.02	14.91	0.02	14.32	0.03	VA
1019.4174	15.89	0.05	15.37	0.03	14.91	0.03	14.29	0.03	GR
1021.3382	16.02	0.02	15.41	0.01	14.96	0.01	14.39	0.02	VA
1025.4611	15.89	0.04	15.35	0.03	14.88	0.03	14.28	0.04	GR
1026.3556	15.89	0.02	15.23	0.01	14.79	0.01	14.24	0.01	VA
1037.4639	16.09	0.10	15.55	0.08	14.97	0.04	14.26	0.05	GR
1039.4326	0.00	0.00	15.62	0.09	15.01	0.03	14.34	0.05	GR
1040.3285	16.05	0.03	15.42	0.02	14.95	0.02	14.34	0.02	VA
1041.4229	0.00	0.00	15.45	0.05	14.98	0.03	14.27	0.03	GR
1042.3438	15.94	0.04	15.37	0.03	14.90	0.02	14.23	0.01	VA
1043.3354	15.87	0.05	15.31	0.03	14.85	0.01	14.20	0.02	VA

Table 3—Continued

JD[a]	B	σB	V	σV	R	σR	I	σI	Tel
1048.3194	15.92	0.03	15.32	0.01	14.86	0.01	14.23	0.01	VA
1050.3146	15.97	0.02	15.34	0.01	14.87	0.01	14.25	0.01	VA
1052.3271	15.91	0.03	15.27	0.02	14.81	0.01	14.18	0.01	VA
1054.4174	0.00	0.00	0.00	0.00	14.72	0.01	14.07	0.03	VA
1057.5313	15.90	0.02	15.22	0.01	14.75	0.01	14.10	0.01	VA
1058.3424	15.86	0.02	15.25	0.02	14.73	0.01	14.10	0.01	VA
1067.2944	16.25	0.05	15.58	0.00	15.10	0.01	14.47	0.01	VA
1072.2847	16.37	0.01	15.71	0.02	15.20	0.01	14.57	0.01	VA
1077.3354	16.45	0.02	15.80	0.02	15.31	0.02	14.68	0.02	VA
1098.2444	16.73	0.03	16.14	0.05	15.69	0.02	15.06	0.01	VA
1100.2979	0.00	0.00	16.27	0.01	15.77	0.01	15.15	0.01	VA
1101.2889	16.86	0.04	16.25	0.03	15.76	0.02	15.13	0.01	VA
1108.2667	0.00	0.00	16.18	0.03	15.70	0.03	15.08	0.03	VA
1109.2410	16.72	0.01	16.18	0.04	15.63	0.02	15.03	0.01	VA
1111.3681	0.00	0.00	15.82	0.01	15.40	0.01	14.78	0.01	VA
1114.2347	16.28	0.02	15.76	0.02	15.30	0.02	14.70	0.02	VA
1125.2090	15.39	0.03	14.82	0.02	14.38	0.01	13.80	0.01	GR
1126.2056	15.26	0.01	14.73	0.01	14.30	0.01	13.70	0.01	VA
1127.2854	15.15	0.03	14.66	0.02	14.18	0.02	13.63	0.02	MP
1133.2986	15.21	0.02	14.66	0.03	14.20	0.01	13.61	0.01	VA
1135.2083	15.45	0.08	14.88	0.05	14.37	0.03	13.76	0.03	MP
1135.2715	15.44	0.01	14.83	0.03	14.40	0.01	13.80	0.01	VA
1138.3042	15.64	0.02	15.01	0.01	14.58	0.04	13.89	0.03	MP
1151.2493	0.00	0.00	0.00	0.00	14.57	0.02	0.00	0.00	VA
1154.5431	15.86	0.01	15.19	0.03	14.70	0.01	14.10	0.01	VA
1156.2472	0.00	0.00	15.24	0.03	14.73	0.01	14.15	0.01	VA
1160.2583	15.82	0.03	15.14	0.03	14.70	0.03	14.07	0.01	VA
1164.2410	15.76	0.02	15.14	0.02	14.69	0.02	14.07	0.02	VA
1294.4354	0.00	0.00	15.72	0.07	0.00	0.00	0.00	0.00	GR
1320.5000	0.00	0.00	0.00	0.00	14.62	0.04	0.00	0.00	GR
1327.3444	15.74	0.03	15.12	0.02	14.62	0.03	14.01	0.03	VA
1338.4424	15.26	0.03	14.65	0.03	14.16	0.03	13.56	0.03	GR
1338.4979	15.23	0.05	14.65	0.04	14.17	0.02	13.56	0.02	MP
1339.3847	15.22	0.03	14.55	0.03	14.09	0.03	13.47	0.03	GR
1344.3701	15.11	0.03	14.43	0.03	14.04	0.02	13.33	0.02	GR
1350.4347	15.21	0.03	14.58	0.03	14.10	0.03	13.53	0.03	GR
1353.3701	15.06	0.03	0.00	0.00	14.05	0.03	13.33	0.03	GR
1373.4035	15.27	0.03	14.71	0.03	14.19	0.03	13.58	0.03	GR
1405.3611	16.42	0.08	0.00	0.00	0.00	0.00	14.62	0.06	GR
1414.3722	16.30	0.08	15.73	0.05	15.21	0.03	14.48	0.03	GR
1422.3549	16.70	0.04	16.03	0.04	0.00	0.00	14.76	0.04	GR
1424.3854	16.53	0.06	15.90	0.03	15.40	0.03	14.76	0.03	GR
1428.3278	16.66	0.04	15.99	0.01	15.46	0.01	14.82	0.01	VA
1433.4410	16.56	0.05	0.00	0.00	0.00	0.00	14.81	0.03	GR
1434.3847	16.53	0.06	15.90	0.04	0.00	0.00	14.75	0.03	GR
1435.4042	16.71	0.05	16.12	0.04	0.00	0.00	14.88	0.03	GR
1445.2660	17.04	0.01	16.44	0.02	15.90	0.02	15.25	0.02	VA
1456.3312	16.97	0.09	16.47	0.04	15.88	0.03	15.24	0.04	GR
1457.3306	16.89	0.01	16.32	0.02	15.79	0.02	15.11	0.01	VA

Table 3—Continued

JD[a]	B	σB	V	σV	R	σR	I	σI	Tel
1480.2382	0.00	0.00	16.56	0.03	16.04	0.03	15.43	0.02	VA
1484.2361	0.00	0.00	16.67	0.09	16.03	0.05	15.35	0.05	GR
1491.2243	17.29	0.06	16.66	0.06	16.08	0.03	15.41	0.04	GR
1508.2389	16.71	0.02	16.11	0.02	15.55	0.02	14.93	0.03	MP
1510.3312	0.00	0.00	16.06	0.02	15.68	0.02	15.12	0.02	MP
1520.2917	16.71	0.02	16.07	0.02	15.63	0.02	15.06	0.01	VA
1546.2326	0.00	0.00	16.16	0.04	15.64	0.04	14.96	0.04	GR
1549.4319	0.00	0.00	16.12	0.02	15.63	0.02	14.98	0.02	VA
1556.2347	0.00	0.00	16.01	0.05	15.56	0.04	14.89	0.04	GR
1569.2410	16.58	0.05	15.95	0.03	15.57	0.03	0.00	0.00	GR
1578.3493	0.00	0.00	0.00	0.00	15.45	0.02	0.00	0.00	VA
1606.4215	16.53	0.02	15.95	0.02	15.42	0.02	14.76	0.02	VA
1613.4931	0.00	0.00	15.86	0.02	15.31	0.02	14.62	0.03	VA
1655.3590	0.00	0.00	0.00	0.00	16.82	0.30	0.00	0.00	GR
1688.5451	0.00	0.00	17.19	0.03	16.80	0.03	16.01	0.04	VA
1695.3903	17.71	0.05	0.00	0.00	16.64	0.02	15.97	0.02	VA
1706.3597	0.00	0.00	0.00	0.00	16.57	0.02	0.00	0.00	VA
1717.5007	17.41	0.03	16.70	0.02	16.19	0.02	15.52	0.02	VA
1718.3965	0.00	0.00	16.74	0.05	16.23	0.04	0.00	0.00	GR
1721.4389	0.00	0.00	16.71	0.05	16.16	0.05	0.00	0.00	GR
1722.5472	0.00	0.00	16.79	0.02	16.20	0.02	15.48	0.02	MP
1724.4493	0.00	0.00	16.86	0.05	16.24	0.02	15.51	0.02	MP
1747.3424	0.00	0.00	0.00	0.00	16.25	0.04	0.00	0.00	VA
1749.3236	0.00	0.00	0.00	0.00	16.23	0.02	0.00	0.00	VA
1751.3542	0.00	0.00	0.00	0.00	16.27	0.03	0.00	0.00	VA
1752.3479	0.00	0.00	0.00	0.00	16.28	0.03	0.00	0.00	VA
1754.3458	0.00	0.00	0.00	0.00	16.31	0.02	0.00	0.00	VA
1758.3458	0.00	0.00	0.00	0.00	16.15	0.04	0.00	0.00	VA
1765.3257	0.00	0.00	0.00	0.00	16.46	0.03	0.00	0.00	VA
1768.3118	0.00	0.00	0.00	0.00	16.45	0.04	0.00	0.00	VA
1789.3687	17.38	0.04	16.87	0.02	16.24	0.02	15.64	0.03	MP
1814.5125	0.00	0.00	0.00	0.00	16.78	0.03	0.00	0.00	MP
1838.2986	0.00	0.00	0.00	0.00	16.05	0.05	0.00	0.00	VA
1841.2667	0.00	0.00	0.00	0.00	16.04	0.03	15.36	0.02	VA
1910.2062	0.00	0.00	0.00	0.00	16.47	0.08	0.00	0.00	GR
2012.4583	0.00	0.00	0.00	0.00	17.00	0.05	0.00	0.00	GR
2083.5090	0.00	0.00	0.00	0.00	16.98	0.05	0.00	0.00	VA
2087.3868	0.00	0.00	0.00	0.00	17.02	0.05	0.00	0.00	VA
2093.4472	0.00	0.00	0.00	0.00	17.30	0.08	0.00	0.00	VA
2098.4278	0.00	0.00	0.00	0.00	17.20	0.08	0.00	0.00	VA
2102.4535	0.00	0.00	0.00	0.00	17.22	0.08	0.00	0.00	VA
2103.3951	0.00	0.00	0.00	0.00	17.23	0.08	0.00	0.00	VA
2112.4097	0.00	0.00	0.00	0.00	17.24	0.03	16.43	0.02	GR
2113.3764	0.00	0.00	17.65	0.08	17.19	0.08	16.52	0.05	VA
2115.4042	0.00	0.00	0.00	0.00	17.35	0.08	16.65	0.08	VA
2116.4111	0.00	0.00	0.00	0.00	0.00	0.00	16.43	0.08	GR
2117.4153	0.00	0.00	0.00	0.00	17.18	0.08	16.59	0.06	VA
2119.4056	0.00	0.00	0.00	0.00	17.22	0.06	16.65	0.06	VA
2120.3701	0.00	0.00	0.00	0.00	17.22	0.08	0.00	0.00	VA

Table 3—Continued

JD[a]	B	σB	V	σV	R	σR	I	σI	Tel
2129.3722	0.00	0.00	0.00	0.00	17.12	0.08	16.52	0.05	VA
2141.4139	0.00	0.00	0.00	0.00	16.86	0.05	0.00	0.00	VA
2148.3146	0.00	0.00	0.00	0.00	16.78	0.05	0.00	0.00	VA
2159.3069	0.00	0.00	0.00	0.00	16.85	0.09	0.00	0.00	GR
2164.3736	0.00	0.00	0.00	0.00	16.74	0.02	0.00	0.00	VA
2165.3438	0.00	0.00	17.24	0.08	16.70	0.05	16.07	0.03	VA
2172.3306	0.00	0.00	0.00	0.00	16.83	0.05	0.00	0.00	VA
2174.3521	0.00	0.00	0.00	0.00	16.79	0.05	16.18	0.03	VA
2178.3076	0.00	0.00	0.00	0.00	16.69	0.02	16.02	0.03	VA
2181.3042	0.00	0.00	0.00	0.00	16.65	0.05	0.00	0.00	VA
2194.2715	17.39	0.08	16.76	0.05	16.29	0.03	15.67	0.03	VA
2195.3174	0.00	0.00	0.00	0.00	16.29	0.03	0.00	0.00	VA
2236.2097	17.69	0.03	0.00	0.00	16.55	0.03	15.88	0.03	TE
2286.2333	17.01	0.08	16.38	0.03	15.91	0.03	15.24	0.02	VA
2287.2556	17.08	0.08	16.44	0.03	15.93	0.03	15.27	0.02	VA

[a] JD-2,450,000

[b] The observation on JD 2236 was obtained with the 70 cm telescope of the Collurania-Teramo Observatory by one of us (RN)

Table 4. Near Infrared observations.

dd-mm-yyyy	J	H	K	α_{nir}
23-08-2001	14.99	14.09	13.26	1.26±0.11
24-08-2001	15.06	14.04	13.27	1.36±0.11
26-08-2001	15.00	14.00		

Table 5. Optical spectral slope fits.

JD-2400000	R	α	$\sigma(\alpha)$	χ^2
464.2	15.71	-1.378	0.063	3.037
549.5	15.85	-1.509	0.084	0.060
711.3	14.43	-1.508	0.079	1.356
712.3	14.54	-1.647	0.079	2.529
717.3	14.54	-1.538	0.064	0.031
719.3	14.77	-1.553	0.063	2.169
721.3	14.82	-1.578	0.072	2.340
723.2	15.06	-1.427	0.079	3.299
723.4	14.99	-1.402	0.072	3.556
727.3	15.51	-1.785	0.063	1.751
731.3	15.78	-1.632	0.074	0.154
744.3	15.51	-1.619	0.072	0.998
747.3	15.40	-1.469	0.064	0.534
748.3	15.39	-1.527	0.063	2.307
781.3	15.70	-1.740	0.093	1.830
823.2	15.11	-1.530	0.079	2.322
863.3	15.53	-1.730	0.084	3.715
865.5	15.40	-1.736	0.079	1.805
871.5	15.11	-1.550	0.063	4.092
872.5	15.15	-1.704	0.079	2.906
891.4	15.28	-1.664	0.072	1.813
901.4	15.46	-1.730	0.079	2.407
928.5	14.90	-1.594	0.088	2.859
955.4	14.82	-1.581	0.063	3.455
956.4	14.54	-1.570	0.075	1.581
985.5	15.38	-1.654	0.063	0.254
993.5	14.94	-1.528	0.079	1.151
1001.4	14.64	-1.338	0.063	0.327
1004.4	14.78	-1.295	0.063	1.034
1005.4	14.97	-1.375	0.072	0.033
1008.4	15.11	-1.320	0.064	1.259

Table 5—Continued

JD-2400000	R	α	$\sigma(\alpha)$	χ^2
1013.4	14.94	-1.251	0.084	0.476
1018.4	14.91	-1.341	0.072	0.364
1019.4	14.91	-1.378	0.079	0.737
1021.3	14.96	-1.365	0.072	0.330
1025.5	14.88	-1.361	0.083	0.296
1026.4	14.79	-1.373	0.072	1.831
1037.5	14.97	-1.782	0.152	0.636
1040.3	14.95	-1.502	0.063	0.165
1042.3	14.90	-1.521	0.072	0.931
1043.3	14.85	-1.471	0.079	0.631
1048.3	14.86	-1.469	0.063	0.090
1050.3	14.87	-1.516	0.063	0.102
1052.3	14.81	-1.527	0.063	0.216
1057.5	14.75	-1.632	0.063	0.508
1058.3	14.73	-1.593	0.063	0.222
1067.3	15.10	-1.581	0.079	0.301
1072.3	15.20	-1.631	0.079	0.206
1077.3	15.31	-1.581	0.079	0.101
1098.2	15.69	-1.448	0.084	0.172
1101.3	15.76	-1.541	0.072	0.016
1109.2	15.63	-1.517	0.082	1.100
1114.2	15.30	-1.327	0.072	0.564
1125.2	14.38	-1.317	0.063	0.017
1126.2	14.30	-1.269	0.063	0.484
1127.3	14.18	-1.230	0.063	0.961
1133.3	14.20	-1.339	0.063	0.128
1135.2	14.37	-1.501	0.103	0.172
1135.3	14.40	-1.385	0.063	0.317
1138.3	14.58	-1.552	0.064	0.785
1154.5	14.70	-1.562	0.072	0.789
1160.3	14.70	-1.549	0.063	1.161

Table 5—Continued

JD-2400000	R	α	$\sigma(\alpha)$	χ^2
1164.2	14.69	-1.465	0.063	0.165
1327.3	14.62	-1.542	0.063	0.139
1338.4	14.16	-1.495	0.063	0.120
1338.5	14.17	-1.453	0.082	0.040
1339.4	14.09	-1.556	0.063	0.756
1344.4	14.04	-1.573	0.063	3.000
1350.4	14.10	-1.462	0.063	0.750
1373.4	14.19	-1.491	0.063	0.760
1414.4	15.21	-1.787	0.103	1.155
1424.4	15.40	-1.600	0.084	0.010
1428.3	15.46	-1.705	0.072	0.308
1445.3	15.90	-1.698	0.095	0.334
1456.3	15.88	-1.698	0.116	1.912
1457.3	15.79	-1.727	0.093	0.512
1491.2	16.08	-1.795	0.120	0.350
1508.2	15.55	-1.645	0.072	1.028
1520.3	15.63	-1.363	0.079	0.726
1606.4	15.42	-1.661	0.084	0.568
1717.5	16.19	-1.750	0.089	0.197
1789.4	16.24	-1.710	0.088	4.749
2194.3	16.29	-1.600	0.103	1.084
2286.2	15.91	-1.671	0.091	0.989
2287.3	15.93	-1.740	0.091	0.837

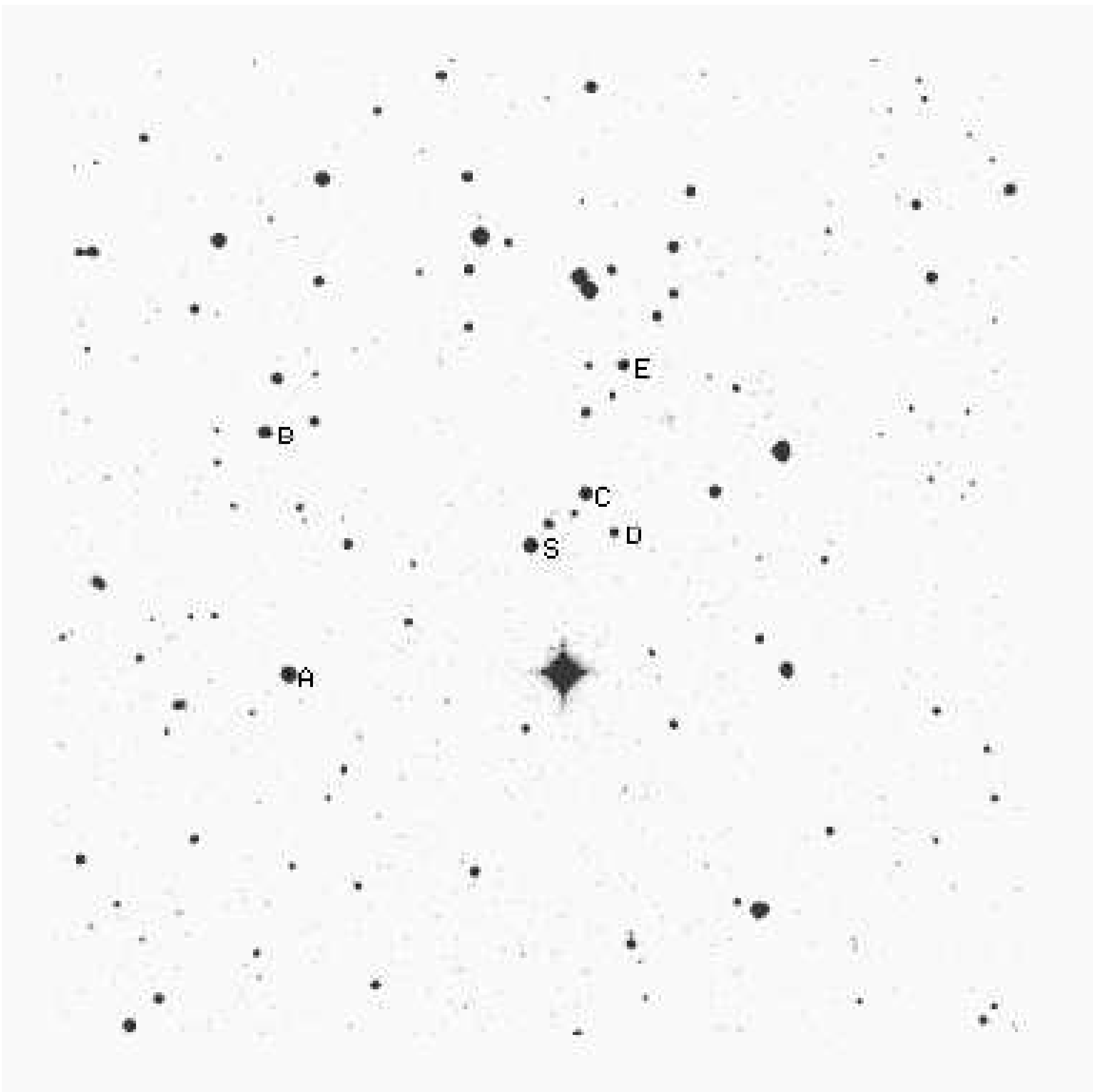
E
B
C
D
S
A

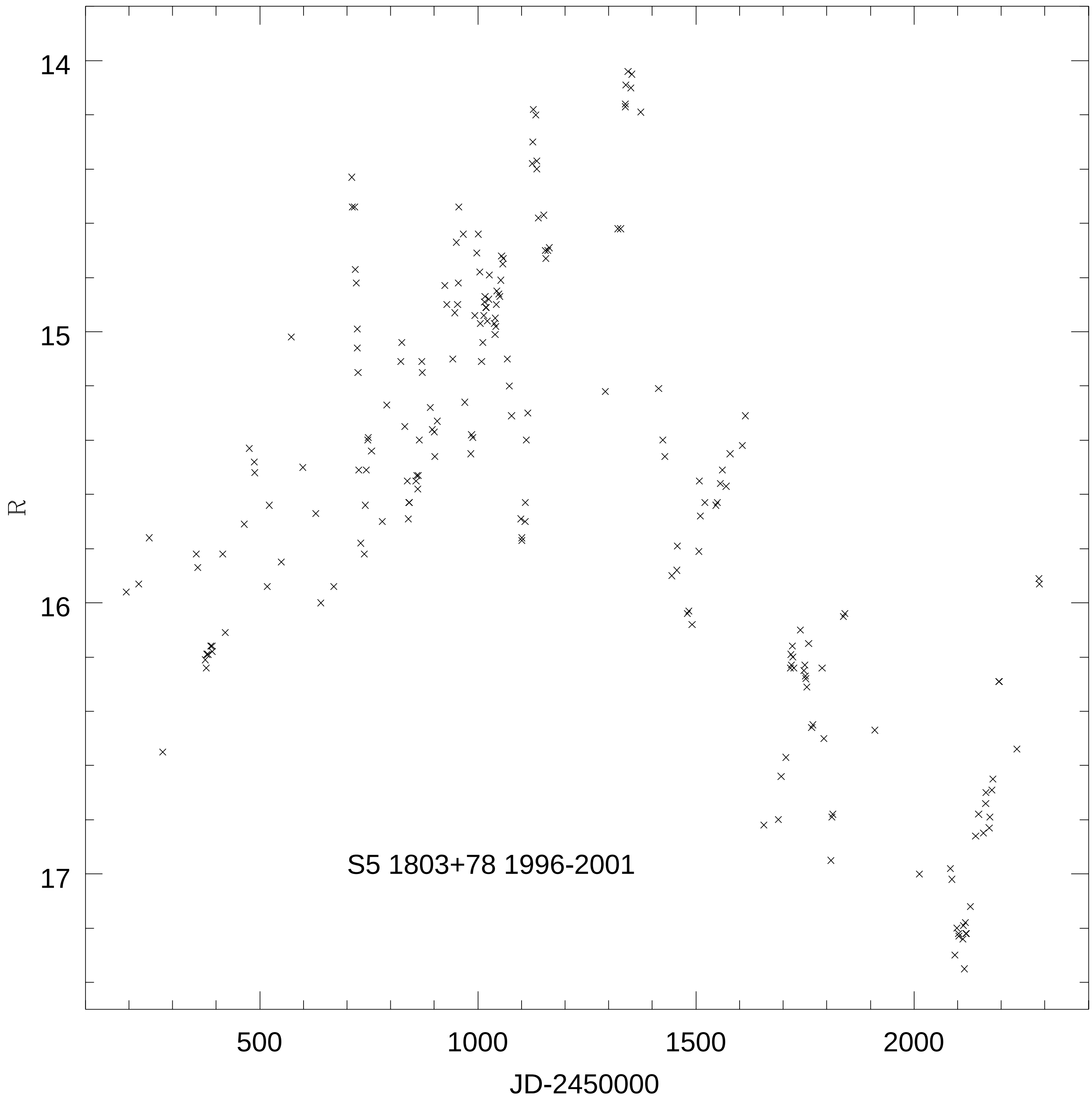

14
15
16
17
R
500
1000
1500
2000
JD-2450000
S5 1803+78 1996-2001

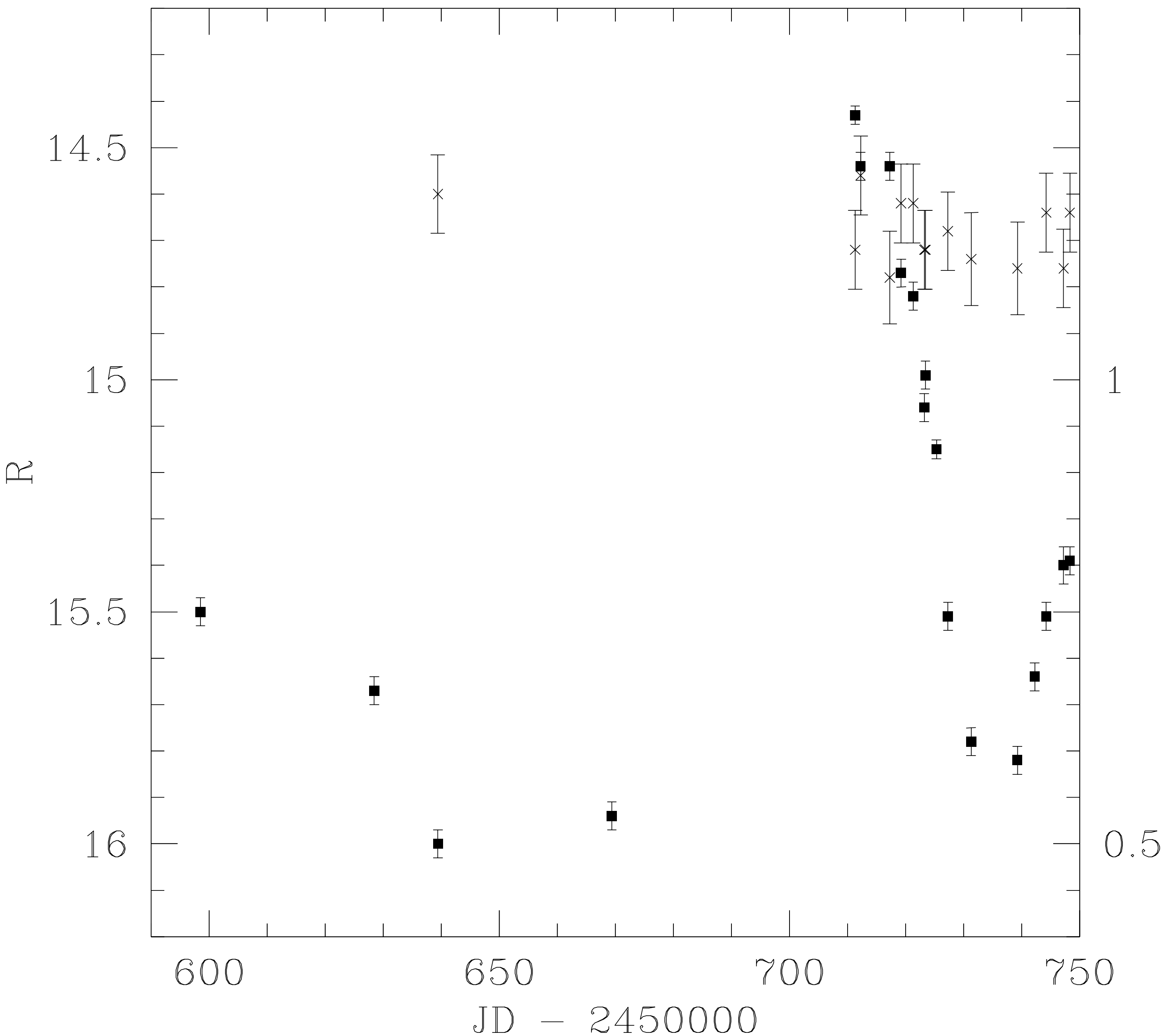

14.5
15
15.5
16
1
0.5
R
600
650
700
750
JD − 2450000

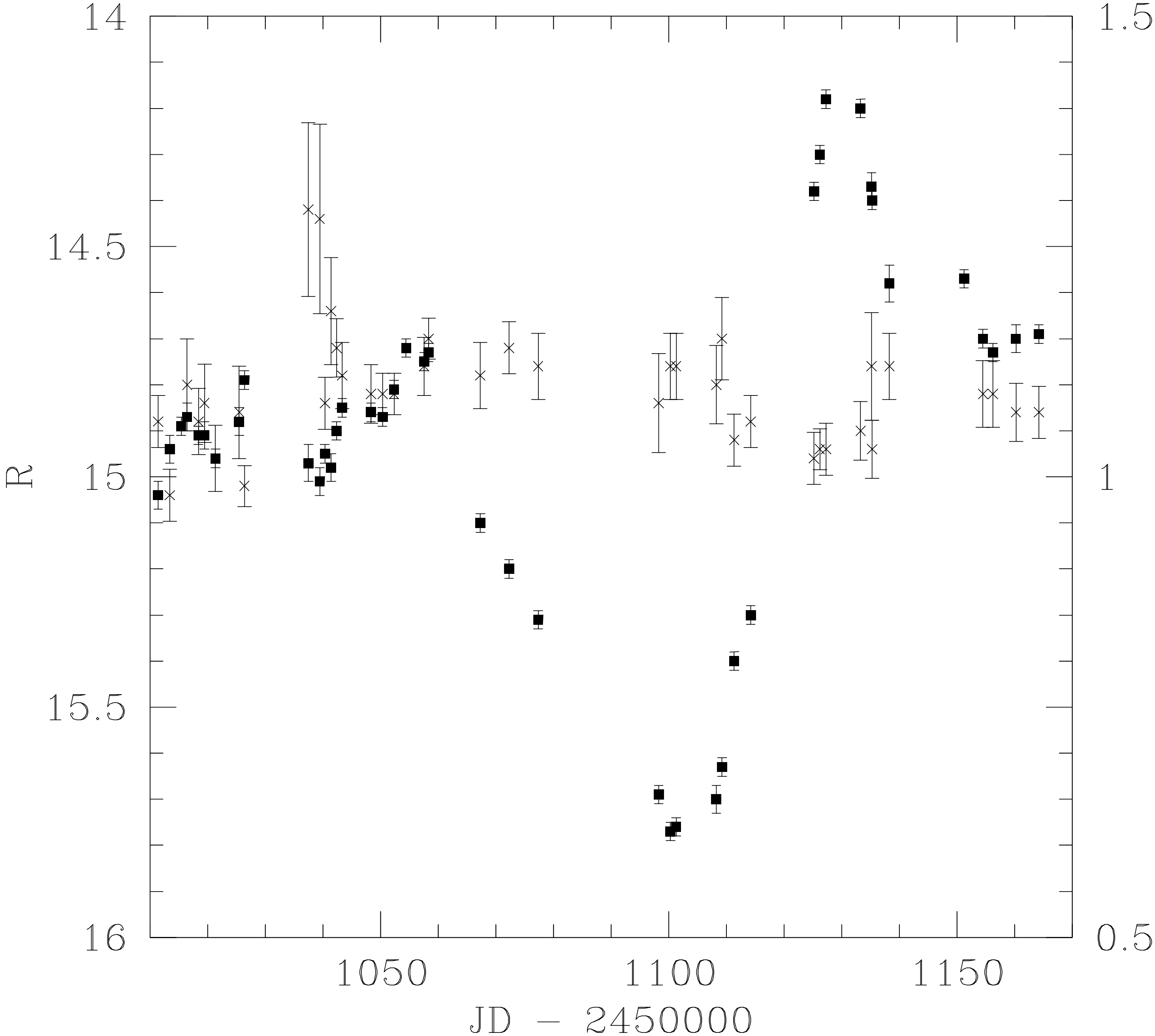
14
14.5
15
15.5
16
1.5
1
0.5
1050
1100
1150
R
JD − 2450000

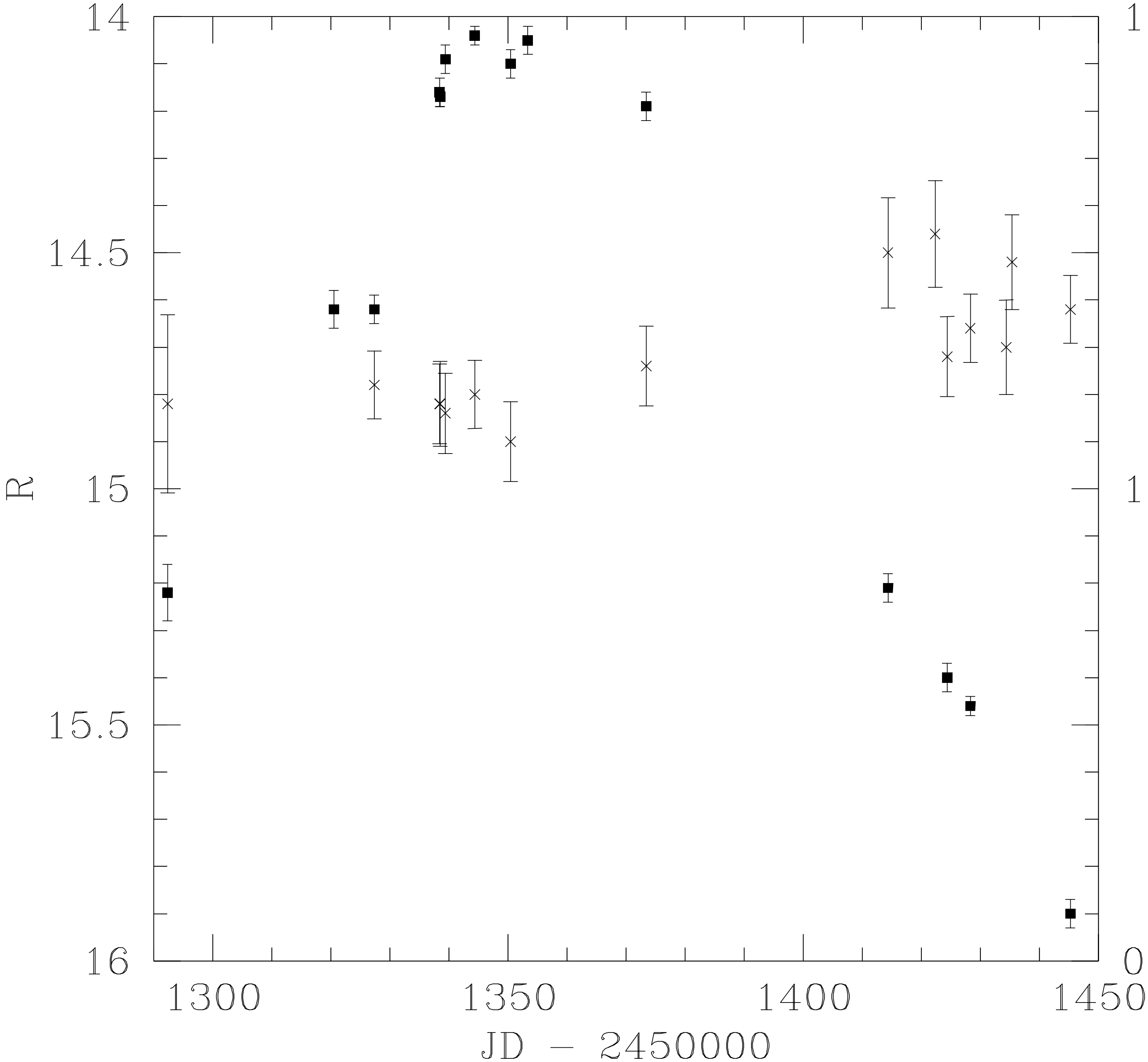

R
JD − 2450000
14
14.5
15
15.5
16
1.5
1
0.5
1300
1350
1400
1450

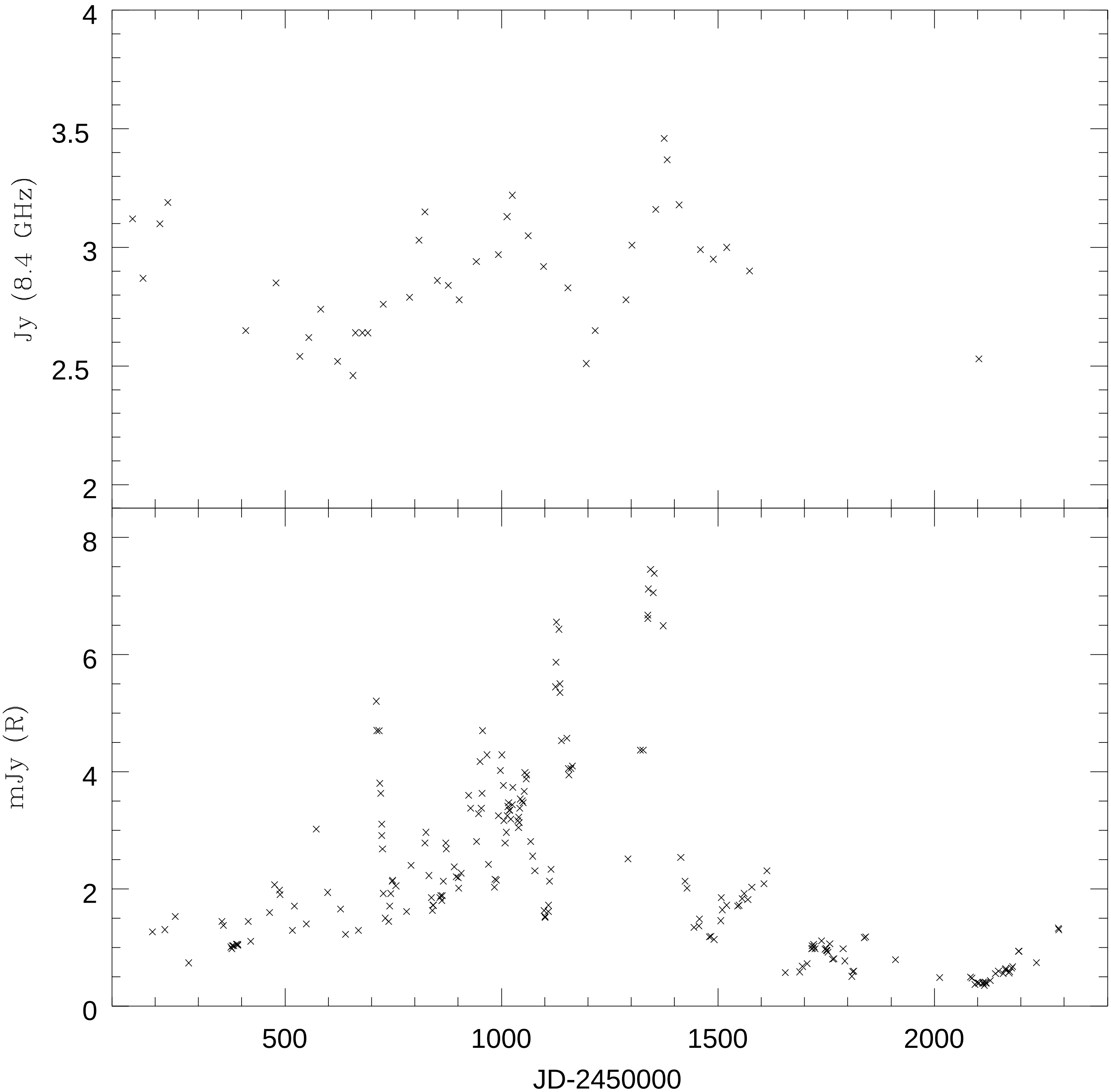

Jy (8.4 GHz)
mJy (R)
JD-2450000
4
3.5
3
2.5
2
8
6
4
2
0
500
1000
1500
2000

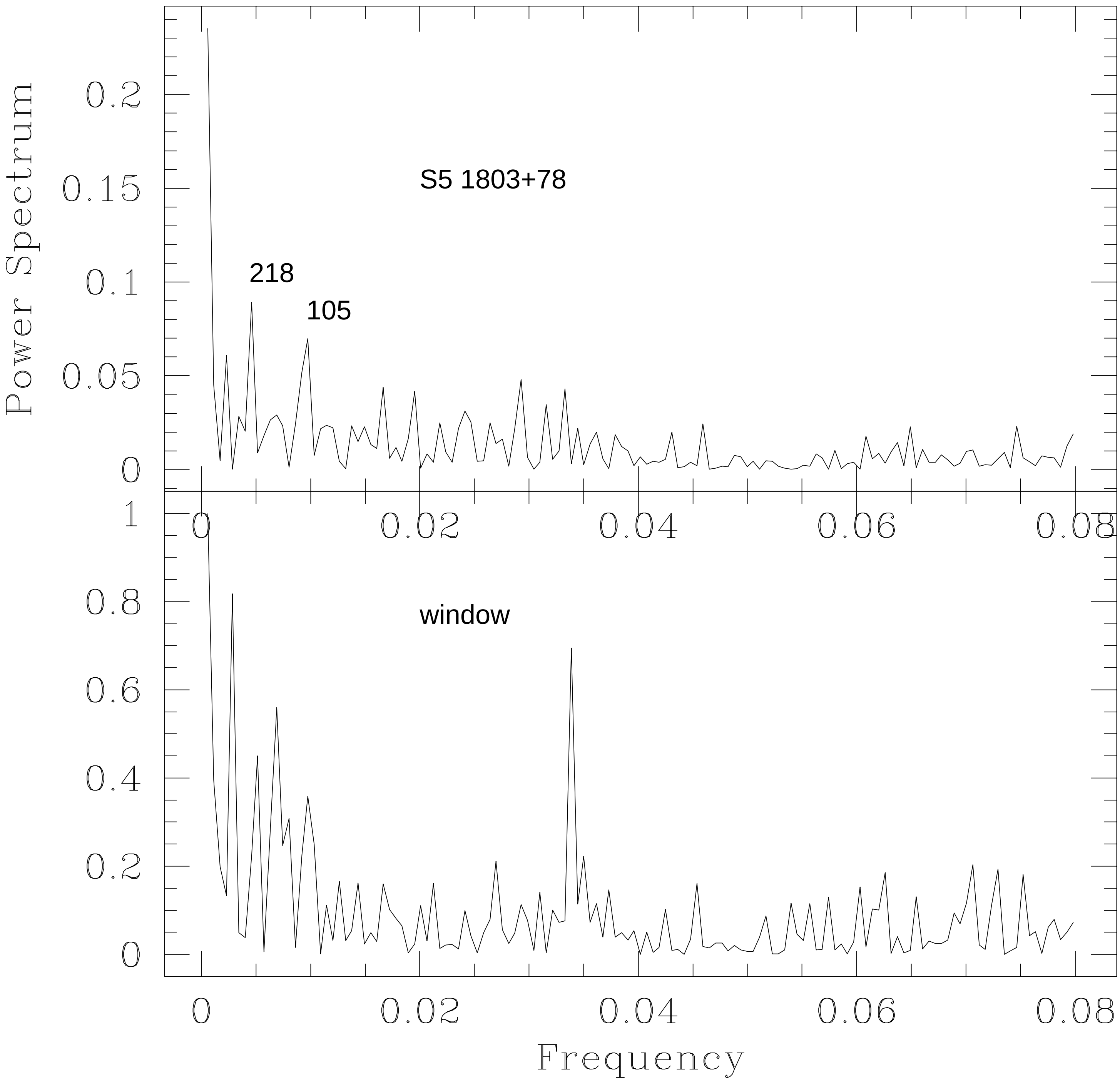
Power Spectrum
S5 1803+78
218
105
window
Frequency
0.2
0.15
0.1
0.05
0
1
0.8
0.6
0.4
0.2
0
0
0.02
0.04
0.06
0.08

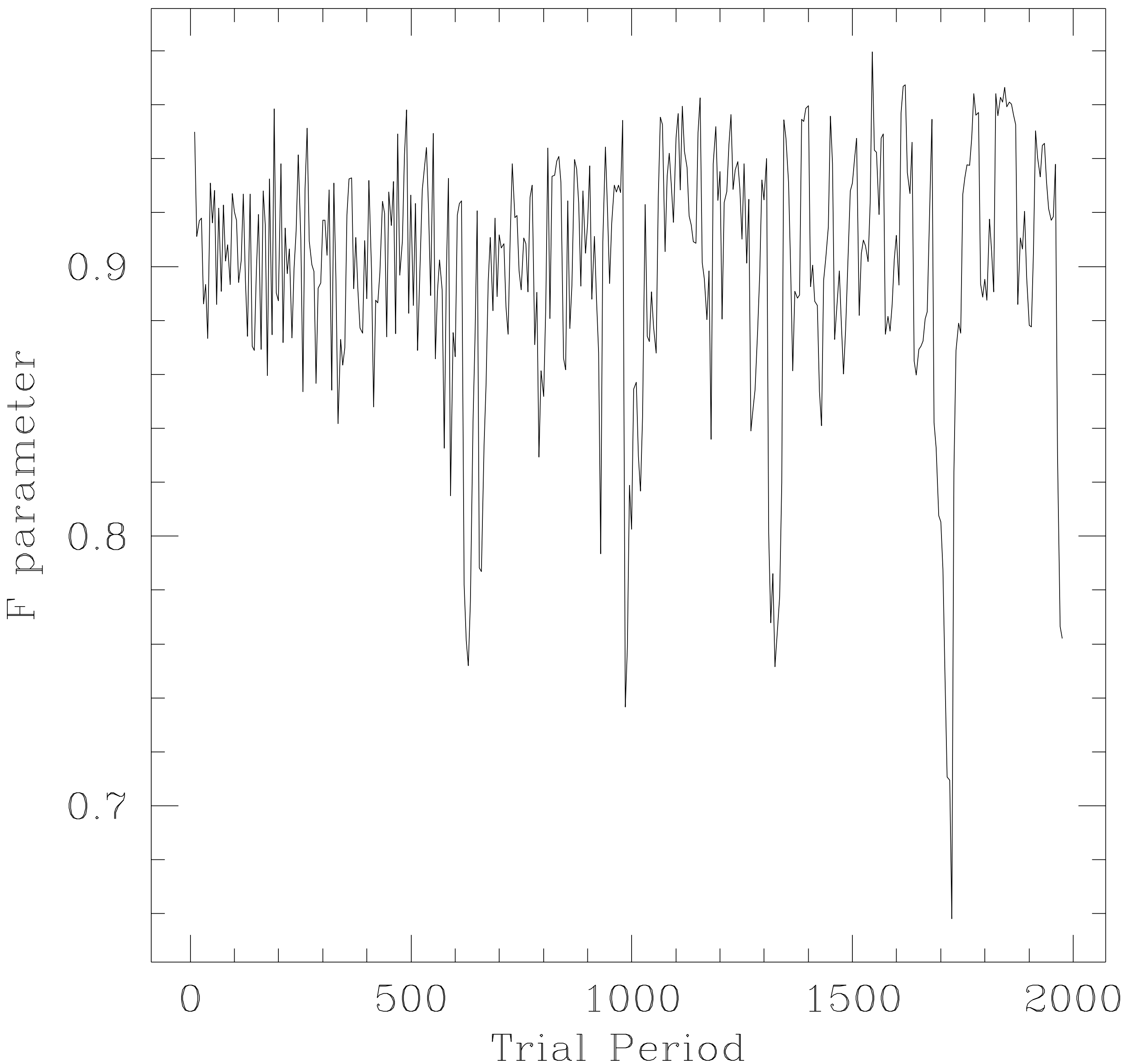

0.7
0.8
0.9
F parameter
0
500
1000
1500
2000
Trial Period

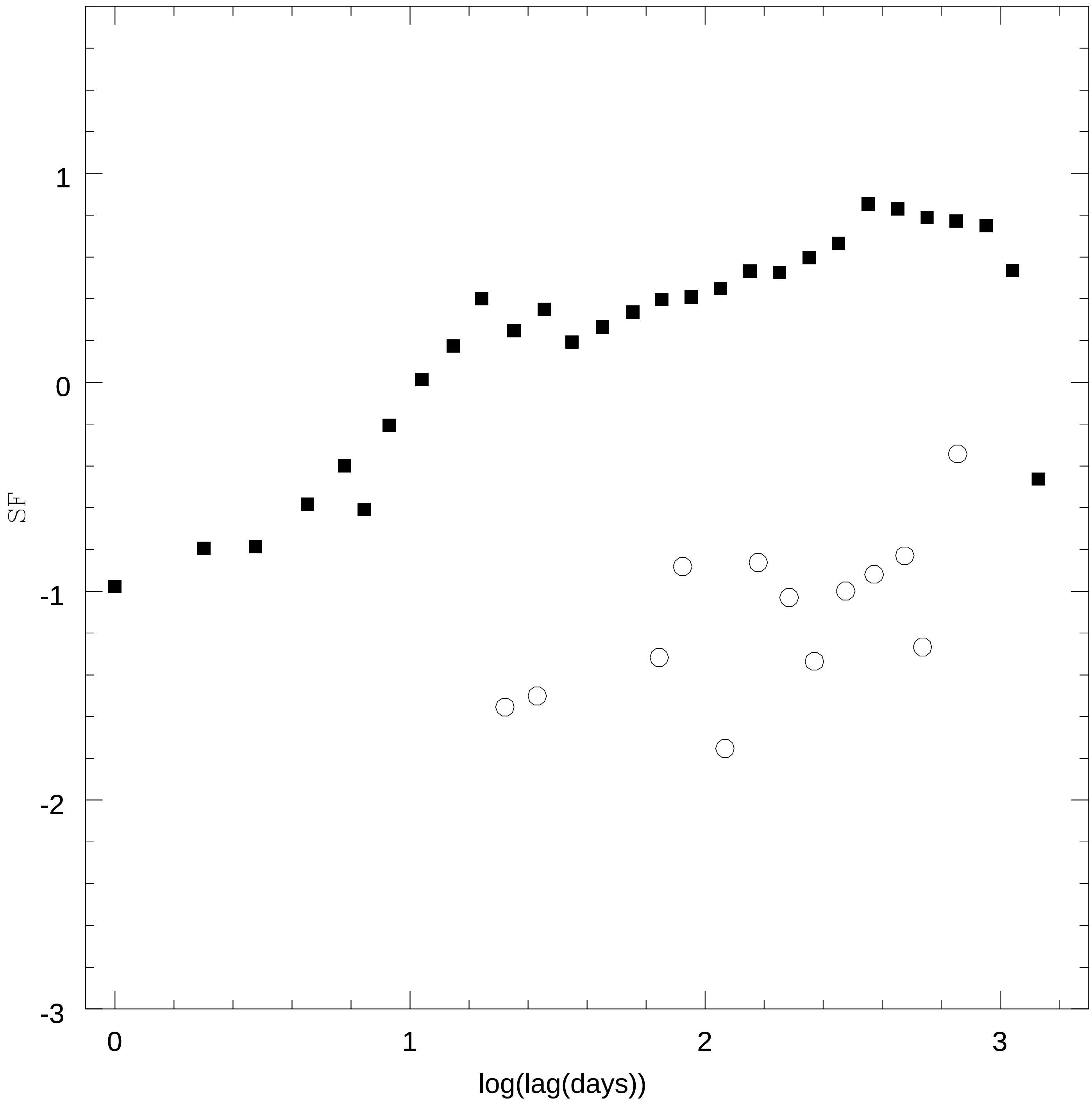

1
0
-1
-2
-3
SF
0
1
2
3
log(lag(days))

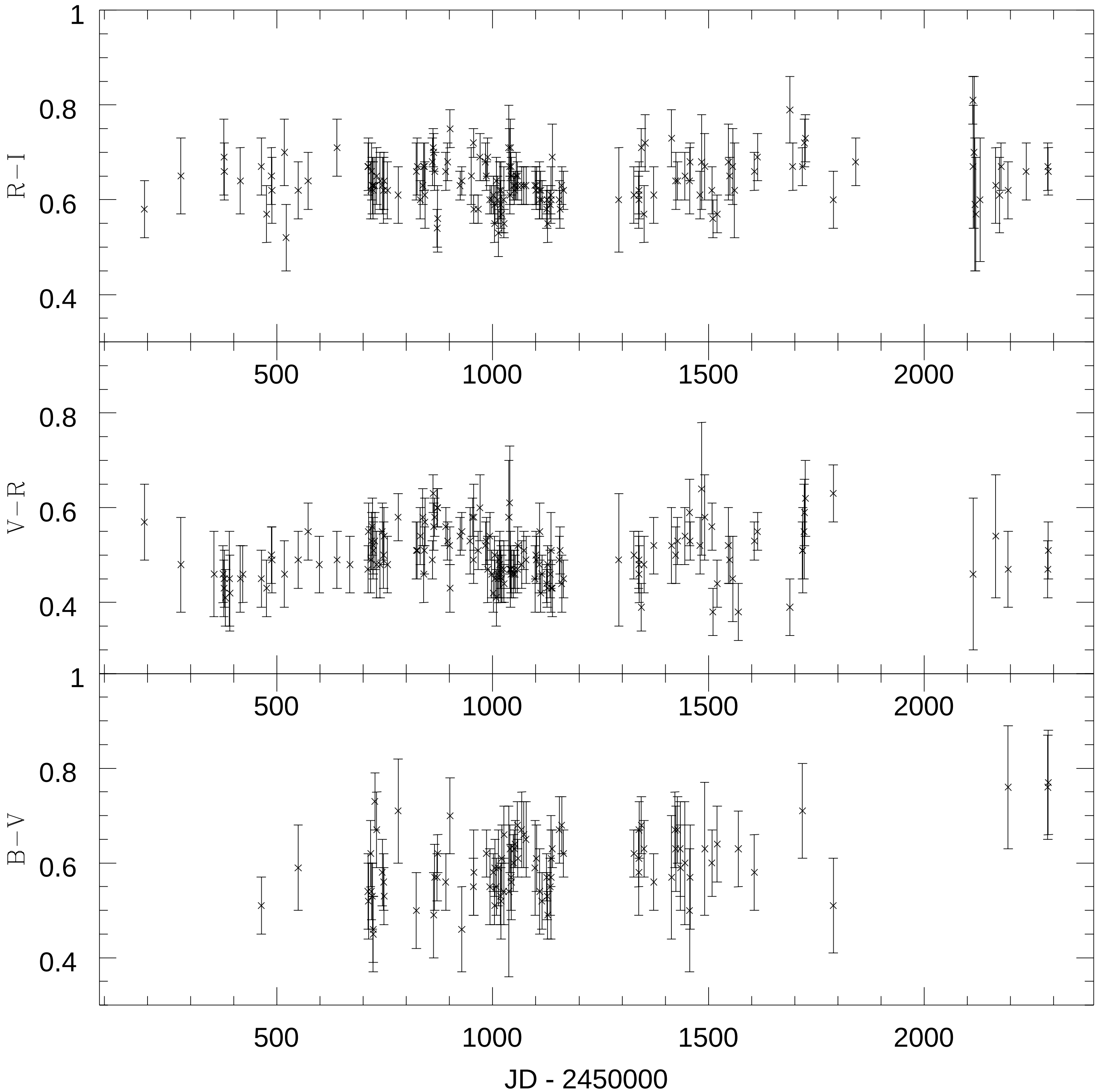

R − I
V − R
B − V
1
0.8
0.6
0.4
500
1000
1500
2000
JD - 2450000

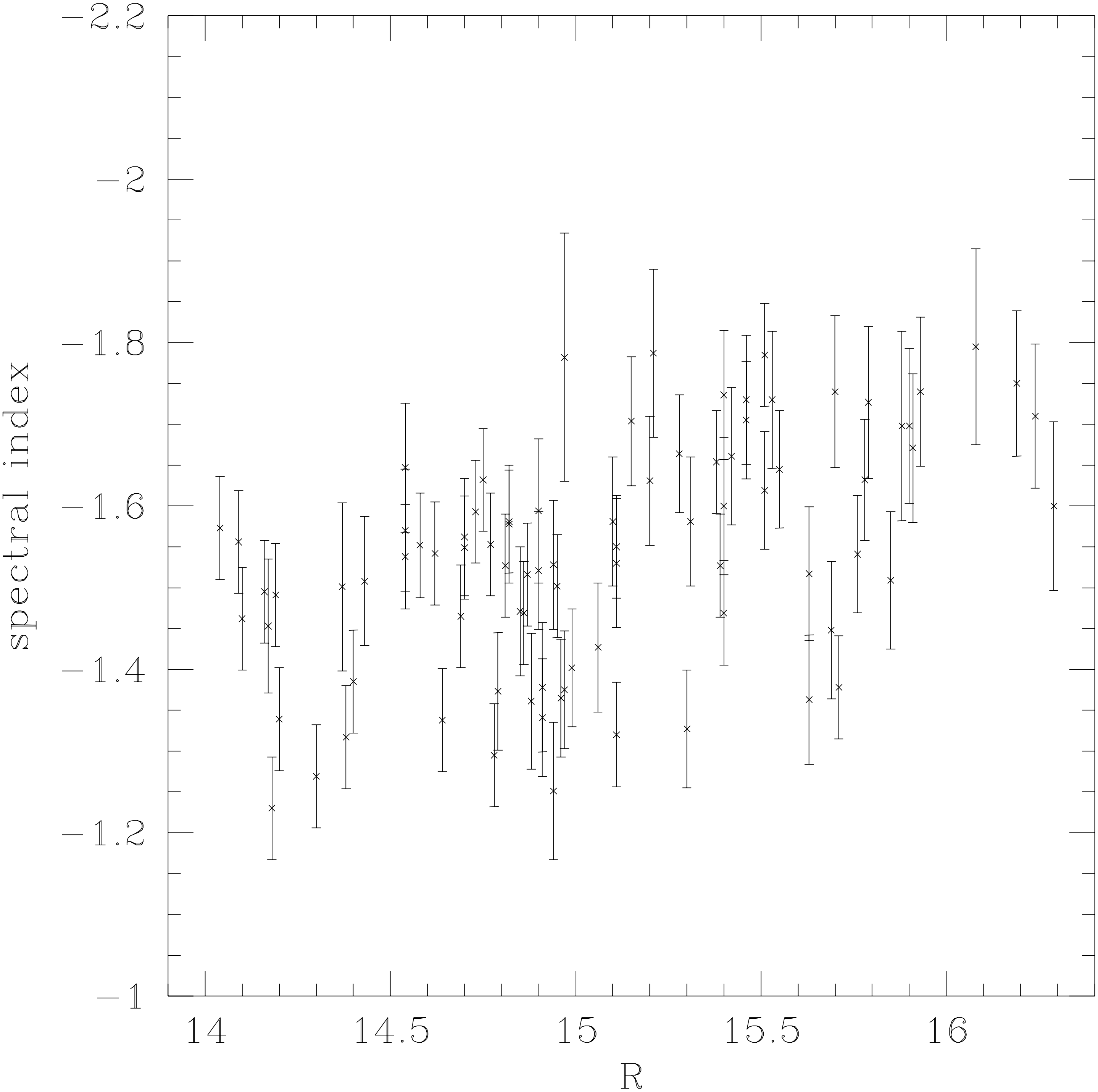

−2.2
−2
−1.8
−1.6
−1.4
−1.2
−1
spectral index
14
14.5
15
15.5
16
R

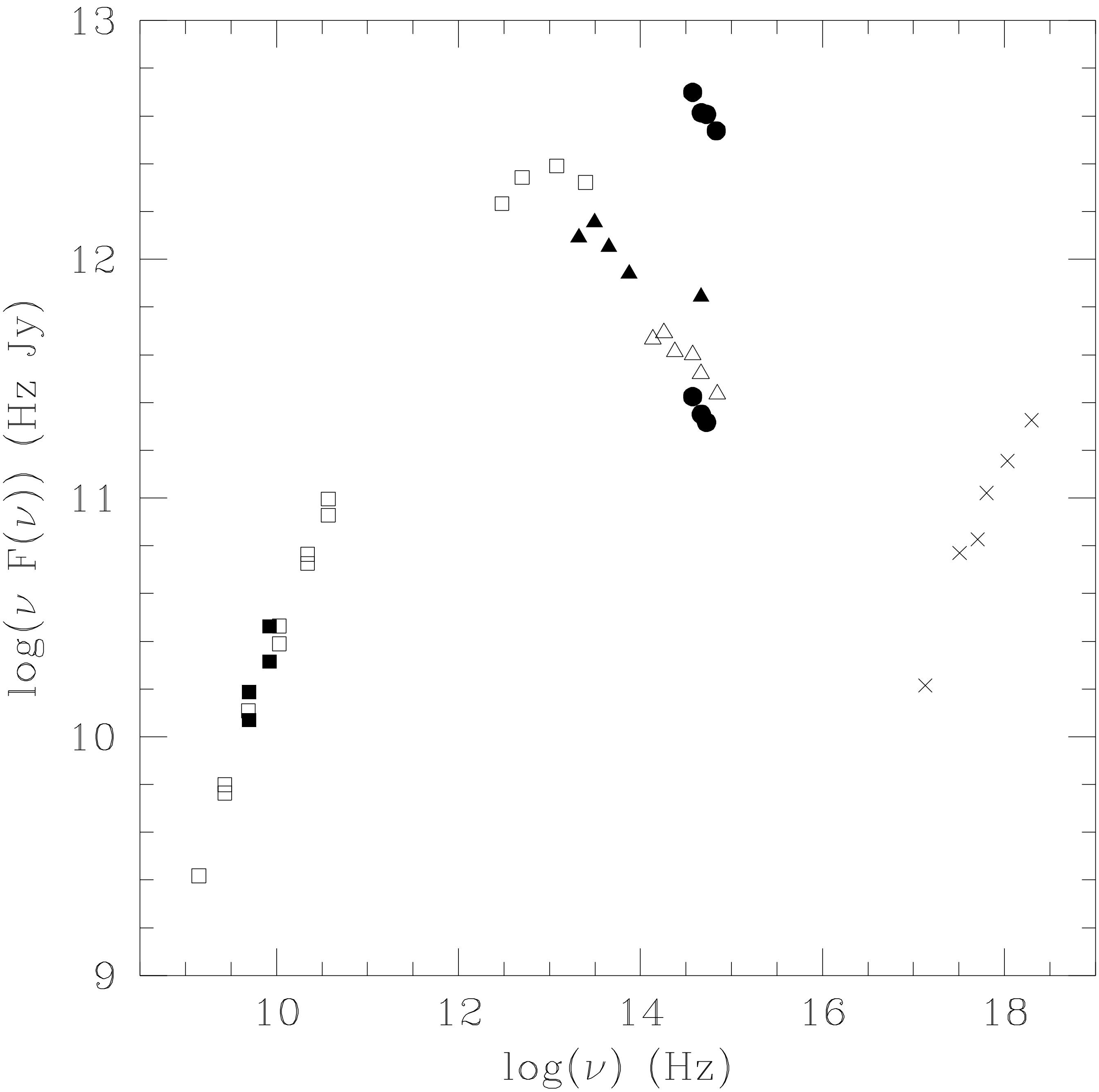

13
12
11
10
9
log(ν F(ν)) (Hz Jy)
10
12
14
16
18
log(ν) (Hz)